Chinese Journal of Polar Science, Vol. 19, No. 2, 149 - 158, December 2008

A coupled multi-category sea ice model and POM for Baffin Bay and the Labrador Sea

Tang Zhili

Bedford Institute of Oceanography, Fisheries and Oceans Canada, Dartmouth, NS, Canada

Received September 20, 2008

Abstract An overview of the seasonal variation of sea-ice cover in Baffin Bay and the Labrador Sea is given. A coupled ice-ocean model, CECOM, has been developed to study the seasonal variation and associated ice-ocean processes. The sea-ice component of the model is a multi-category ice model in which mean concentration and thickness are expressed in terms of a thickness distribution function. Ten categories of ice thickness are specified in the model. Sea ice is coupled dynamically and thermodynamically to the Princeton Ocean Model. Selected results from the model including the seasonal variation of sea ice in Baffin Bay, the North Water polynya and ice growth and melt over the Labrador Shelf are presented.

Key words Baffin Bay, Labrador Sea, sea ice model.

1 Introduction

The seasonal variation of sea-ice cover in Baffin Bay and the Labrador Sea is primarily a response to atmospheric forcing. Early attempts to model the sea ice employed Hibler's (1979)[1] two-category ice model without an ocean model or with a diagnostic ocean model (Ikeda *et al.* 1988, Tang and Gui 1996)[2,3]. To represent the ocean more realistically, the Bryan-Cox ocean model (Bryan 1969, Cox 1984)[4,5] was coupled to the Hibler model by Ikeda *et al.* (1996)[6]. The coupled model was able to reproduce the interannual variability among the light, medium and heavy ice seasons. A major improvement of the ice model was made by Yao *et al.* (2000a)[7] who developed a multi-category ice model, and coupled it to the Princeton Ocean Model (POM). The coupled model has been used to study short-term ice movement (Yao *et al.* 2000b)[8], North Water polynya (Yao and Tang 2003)[9], seasonal variation of sea ice and related ice-ocean processes (Yao *et al.* 2000a, Tang and Dunlap 2007, Dunlap *et al.* 2007)[7,10,11], transport and circulation in Baffin Bay (Tang *et al.* 2004, Dunlap and Tang 2006)[12,13], and wave-current interaction (Tang *et al.* 2007)[14]. The model has also been used in operational ice-ocean forecasting (website: http://www.mar.dfo-mpo.gc.ca/science/ocean/icemodel/forecast.html). The coupled model is designed for any ice covered ocean. It has been adapted for the Arctic Ocean and northern North Atlantic by Wang *et al.* (2005)[15] to study large-scale atmosphere-ocean interaction (Wang *et al.* 2004)[16]. Several versions of the coupled model with different coverage and coordinate system have been implemented. The latest version, called CECOM (Cana-

dian East Coast Ocean Model), has a model domain extending from Baffin Bay to the Gulf Stream, and employs the generalized σ and rotated spherical coordinates.

In this paper, an overview of sea-ice conditions in Baffin Bay and the Labrador Sea is given, and the formulation of CECOM is outlined. Selected results from modelling studies of the region using the coupled model including the seasonal variation of sea ice in Baffin Bay, North Water polynya and ice growth and melt over the Labrador Shelf are presented. Future developments and applications are discussed.

2 Seasonal variation of sea ice cover

In a typical ice year, sea ice appears off the northwestern coast of Baffin Bay in early October. With the progression of the season, the ice cover increases in size and spreads southwards along the coast of Baffin Island and eastwards to central Baffin Bay. By mid-November, ice covers all areas west of 60°W. Ice reaches the northern Labrador coast in January, and extends southward along the Labrador coast until the end of March when the ice reaches its southernmost position at 47°N on average before starting to retreat north. By mid-July, the Labrador Shelf is clear of ice. In Baffin Bay, ice area continues to decrease through summer and by early September Baffin Bay becomes ice free. Figs. 1 and 2 show

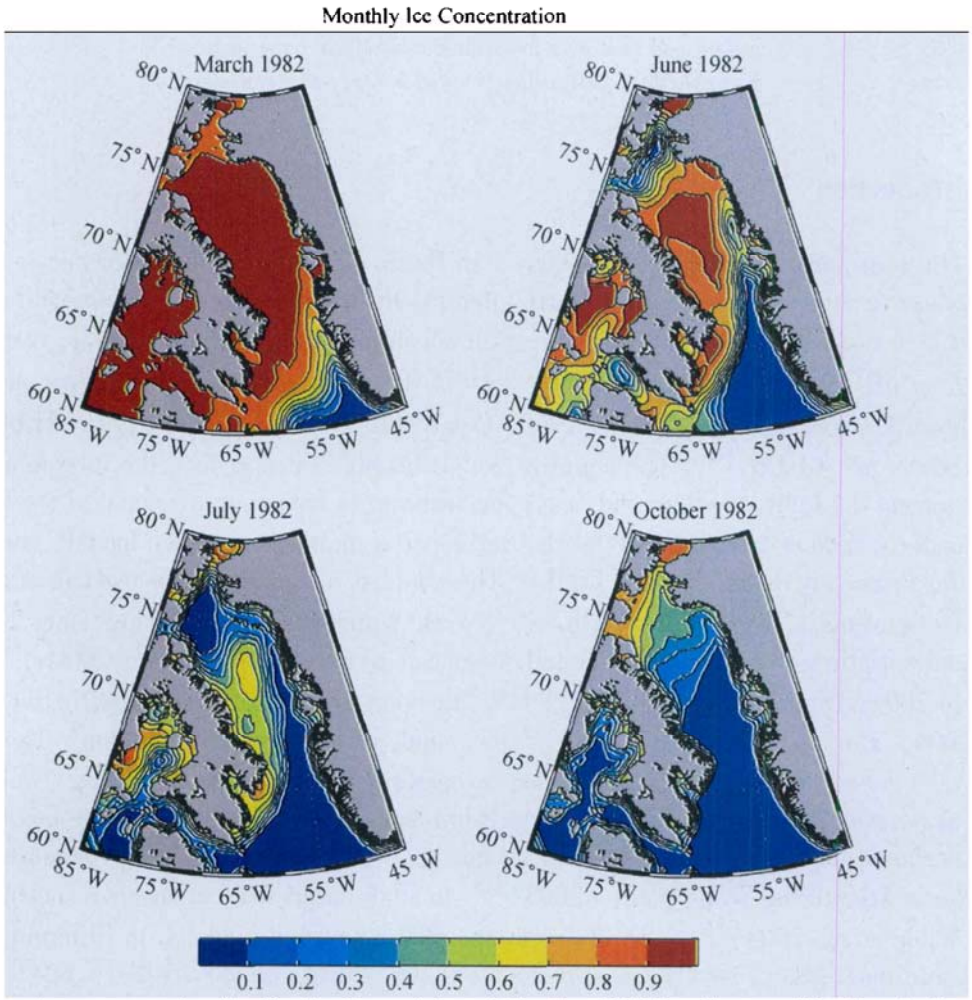

Fig. 1 Mean ice concentration for March, June, July and October 1982 based on satellite data (taken from Tang *et al.* 2004[12]).

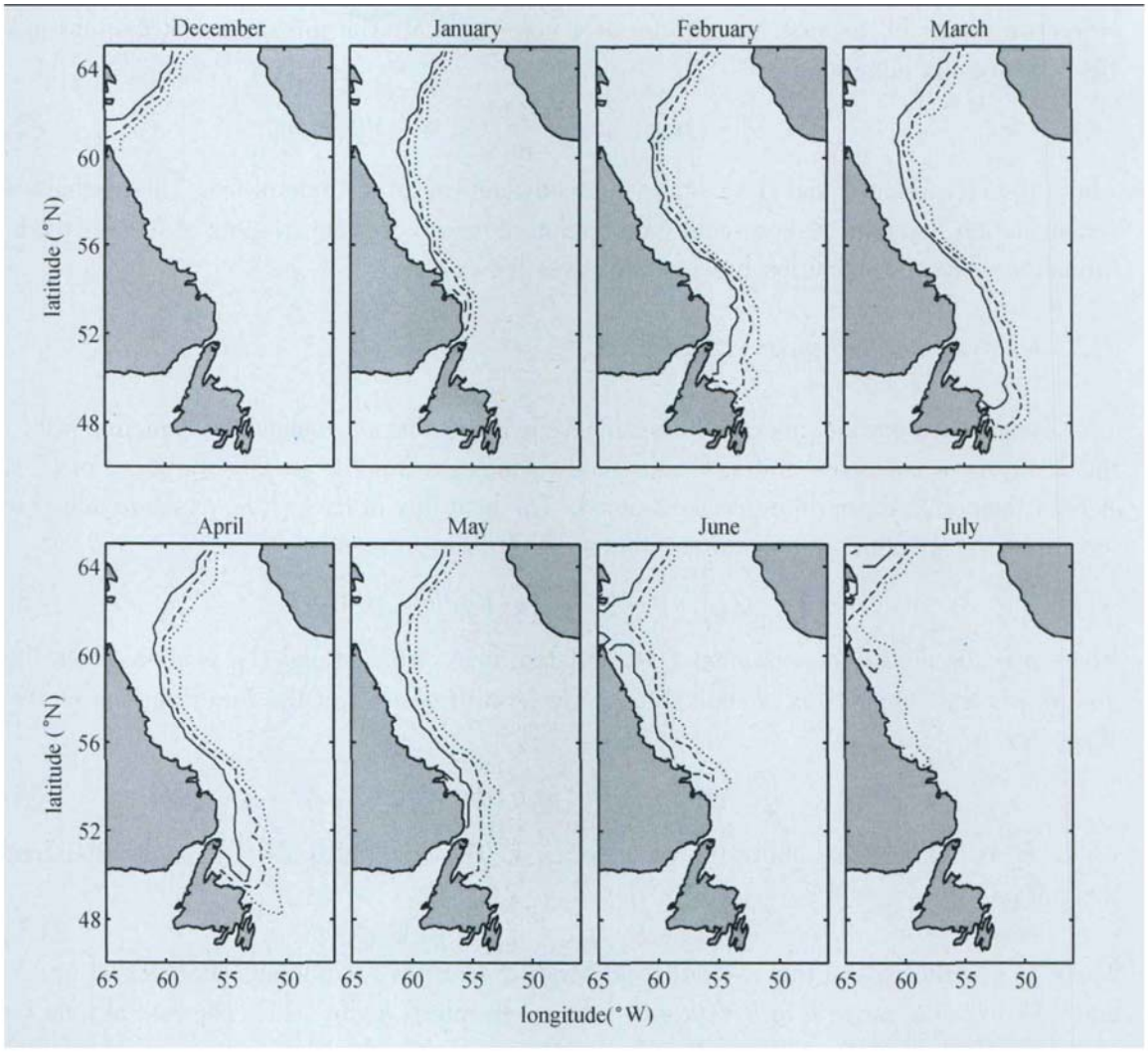

Fig. 2 The seasonal evolution of observed ice concentration (taken from Yao *et al.* 2000[7,8]). Concentrations are shown for the beginning of the indicated months. The contours are 0.1 (dotted line), 0.5 (dashed line), and 0.9 (solid line).

the annual cycle of ice cover in Baffin Bay and the Labrador Sea based on satellite data and reconnaissance flights (Yao *et al.* 2000, Tang *et al.* 2004)[7,8].

3 Description of CECOM

3.1 Ice thickness distribution

The formulation of the multi-category sea ice model follows Thorndike *et al.* (1975)[17] and Hibler (1980)[18]. The presence of open water with ice of various thicknesses is characterized with a thickness distribution $g(h)$ where $g(h)\,dh$ is defined as the fraction of area covered by ice between thicknesses h and $h+dh$. Ice-covered fraction A and mean ice thickness $\bar{h}$ are defined from $g(h)$ as

$$A = \int_{0+}^{\infty} g(h)\,dh \qquad \bar{h} = \int_{0}^{\infty} hg(h)\,dh \tag{1}$$

where the limits in the first integral are over non – zero h. The thickness distribution satisfies a continuity equation

$$\frac{\partial g}{\partial t} + \nabla \cdot (\boldsymbol{u}_i g) = -\frac{\partial (fg)}{\partial t} + \Psi + diffusion \tag{2}$$

where $\boldsymbol{u}_i$ is ice velocity and $f(h)$ is the thermodynamical growth rate of ice. The mechanical redistribution function Ψ represents the creation of open water and ridging of ice during deformation. The redistribution process conserves ice volume.

3.2 *Ice dynamics and thermodynamics*

The momentum balance governing ice velocity is the ice momentum equation with a quadratic ice-ocean stress term. Ice thermodynamics governs the growth rate $f(h)$ in (2). A liner temperature profile in ice is assumed. The heat flux in ice, $Q(h)$, is determined by ice surface and bottom temperatures. Surface melt is expressed as

$$\int_{0+}^{\infty} [Q_{AI}(h) - Q(h)] g(h) dh = \rho L W_{AI} \tag{3}$$

where ρ is the density of seawater, L is the latent heat of fusion and Q_{AI} is air-ice heat flux and W_{AI} is the volume flux of melt water. The growth or melt at the lower surface of ice, W_{IW}, is

$$\int_{0+}^{\infty} [Q(h) - F_T] g(h) dh = \rho L W_{IW} \tag{4}$$

where F_T is the heat flux out of the ocean surface. The ice growth over the open water fraction, W_{AW}, is

$$(Q_{AW} - F_T)(1 - A) = \rho L W_{AW} \tag{5}$$

where Q_{AW} is the air-sea flux excluding penetrating shortwave radiation. The integral in (3) and (4) over the range h to $h + dh$ give the growth rate $f(h)$ in (2). The rate of total ice growth is given by $(W_{AI} + W_{IW} + W_{AW})\rho/\rho_i$ where ρ_i is the density of ice.

Snow is not modeled in CECOM. We specify the thin ice ($h < 0.2$ m) is bare ice with an albedo of 0.5 and thicker ice is snow-covered with an albedo of 0.75. The presence of snow has no other effect except to modify the albedo.

3.3 *Ice-ocean coupling*

Heat and salt fluxes at the ice-ocean interface are governed by the boundary processes discussed by Mellor and Kantha (1989)[19]. The heat flux out of the ocean is

$$F_T = -\rho c_p C_T (T_0 - T) \tag{6}$$

where c_p is the specific heat of seawater, T_o is the temperature at the lower surface of ice and T is the ocean temperature under ice. The heat transfer coefficient, C_T, is a function of the friction velocity and the roughness length. The salt flux out of the ocean is

$$F_S = (W_{AI} + W_{IW} + W_{AW})(S_I - S) + (1 - A)S(P - E) \tag{7}$$

where S_I is the salinity of ice, S is the salinity under ice, P is precipitation and E is evaporation.

Analogous to the heat flux (6), the salt flux is defined

$$F_S = -C_S (S_0 - S) \tag{8}$$

where S_0 is the salinity at the ice-ocean interface. The salt transfer coefficient C_S is a function of the friction velocity and the roughness length.

Given the heat flux $Q(h)$ from the ice model, (3) to (8) are solved for F_T, F_S, $(W_{AI} + W_{IW} + W_{AW})$, T_0 and S_0 under the constraint that T_0 is the freezing temperature at salinity S_0. In open ocean, the constraint is relaxed and F_T is set equal to Q_{AW}.

3.4 Ocean model

The ocean component of CECOM is based on the Princeton Ocean Model which has been fully described in Blumberg and Mellor (1987)[20]. The major modification in CECOM is an additional term in the temperature equation to allow penetrating shortwave radiation in ice free waters only:

$$\frac{\partial T}{\partial t} + u\frac{\partial T}{\partial x} + v\frac{\partial T}{\partial y} + w\frac{\partial T}{\partial z} = \frac{\partial}{\partial z}\left(K_H\frac{\partial T}{\partial z}\right) + \frac{1-A}{\rho c_p}\frac{\partial I}{\partial z} + \textit{horizontal diffusion}$$

where K_H is the vertical eddy diffusivity and I is the penetrating shortwave radiation. Shortwave radiation absorbed at the ocean surface (non-penetrating) is considered part of the total air-sea heat flux.

4 Model implementation

Temperature and salinity data required to initialize the model were obtained from an objective analysis of historical data archived at Bedford Institute of Oceanography dating back to 1910. The analysis employed an iterative difference correction procedure with topography-dependent radii of influence (Tang 2007)[21]. Seasonal and monthly climatologies on a horizontal grid of $1/6° \times 1/6°$ were produced from the analysis. Fig. 3 shows surface temperature in August. Compared to global data sets, this high-resolution data set has a much better representation of temperature and salinity in the shelf and shelf edge regions.

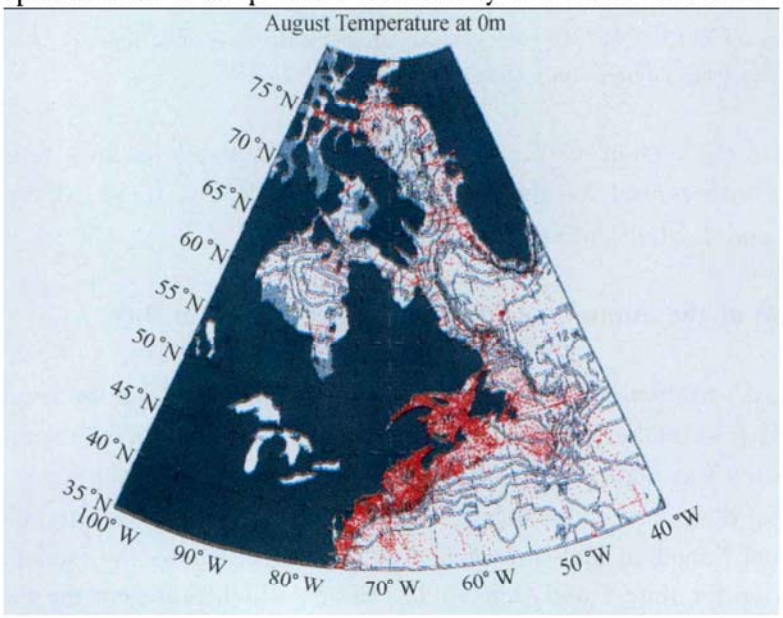

Fig. 3 Sea surface temperature for August. The red dots are locations of raw data.

To reduce the impact of converging meridians, a rotated coordinate system was used in CECOM in which the rotated equator bisects the domain. The horizontal resolution is 1/10° ×1/10°. The area of coverage is shown in Fig. 4. In the vertical, the generalized-σ coordinates are implemented in order to increase the vertical resolution of the upper ocean in areas of large water depth (Fig. 5). At open boundary, the flow relaxation scheme of Martinsen and Engedahl (1987)[22] is used. For temperature and salinity, monthly or seasonal means are prescribed. For velocity, the barotropic component is derived from prescribed transports. The baroclinic component is determined from geostrophy.

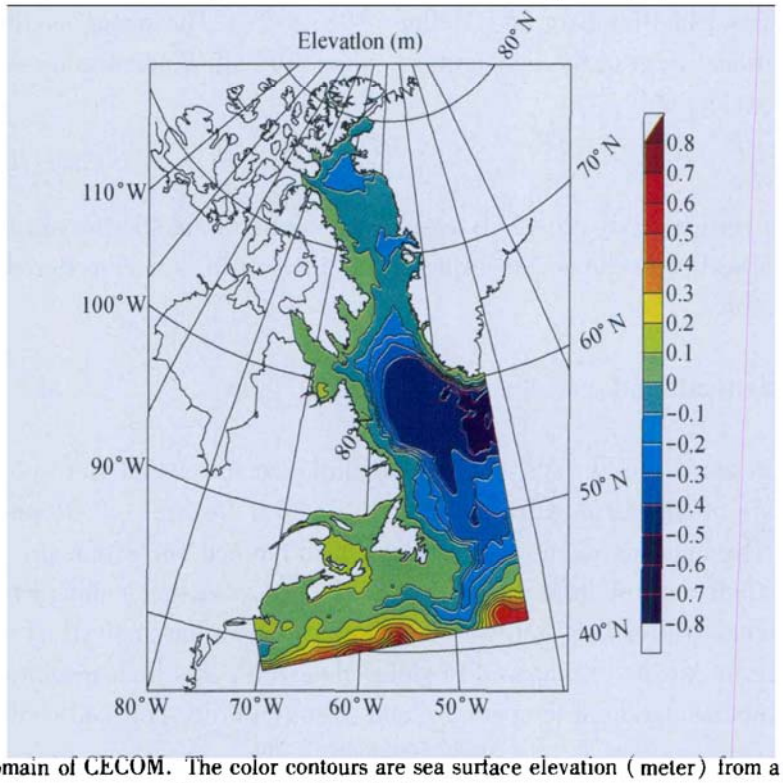

Fig. 4 Model domain of CECOM. The color contours are sea surface elevation (meter) from a spinup run of the model using temperature-salinity climatology for October.

In the discrete version of (2), an ice category includes ice in a range of thickness. Ten categories with central ice thickness of 0, 0.12, 0.28, 0.52, 0.86, 1.32, 1.91, 2.54, 3.51, and 4.51 m are specified in CECOM.

5 Simulation of the annual variation of sea ice in Baffin Bay

The annual variation of ice cover in Baffin Bay is studied from the result of a 16-month run of CECOM (September 2004 to December 2005). After the model spinup, 3-hourly atmospheric forcing was applied. The heat, moisture fluxes and wind stress were calculated from the air and dewpoint temperatures, surface wind, precipitation, and cloud fraction data obtained from Canadian Meteorological Centre. Fig. 6 shows the modeled and observed ice concentration for June 1 and October 17, 2005, which represent the melting and growing phases of the ice field respectively. The model results are able to capture the major fea-

tures of the ice field. From early January to mid-May, Baffin Bay is completely covered by

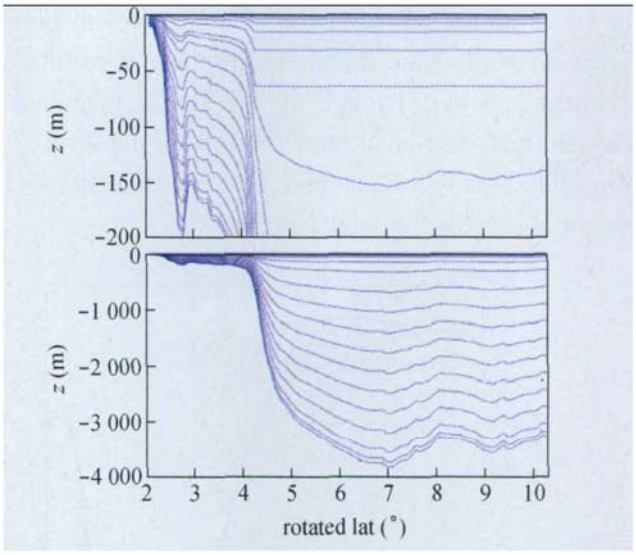

Fig. 5 A cross-section of the generalized coordinates across the Labrador shelf at 55°N. The upper panel shows the coordinates over the upper 200 m.

ice except in the southeastern part of the bay east of 55°W. Ice melting starts in the south in Davis Strait. This is clearly seen in the map of June 1. The map also shows an ice free area in northern Baffin Bay known as the North Water polynya. Ice growth after summer starts in October in Smith Sound. By mid-October, the ice limit reaches 73°N (lower panel of Fig. 6).

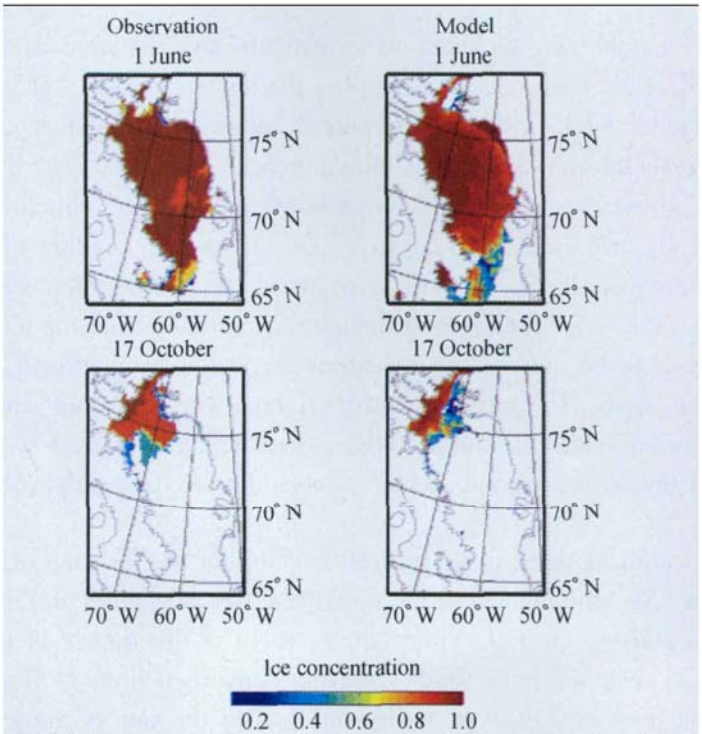

Fig. 6 Observed (left) and modeled (right) ice concentration for June1 and October 17, 2005.

A quantitative model-data comparison of the annual cycle can be made by computing the ice area between 65°N and 80°N (Fig. 7). The agreement between the model simulation and the data is excellent. For ice thickness, the model results (not shown here) indicate that thick ice, up to 2.5 m, is found off the Baffin Island coast in April and May. Long-term near-shore measurement of ice thickness at Clyde River (74.47°N, 67.42°W) on the coast of Baffin Island gives a range of 1.2 – 2.2 m at the end of May (Tang *et al.*, 2004), which is comparable with the model prediction.

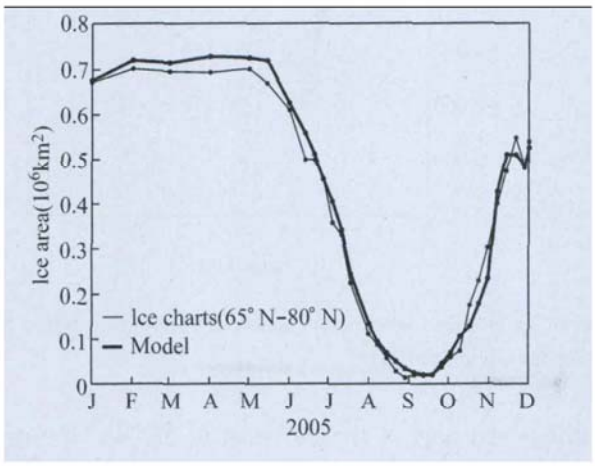

Fig. 7 Comparison of ice area between 65°N and 80°N from data and model (taken from Tang and Dunlap 2007[10]). The tick marks and month labels indicated the beginning of each month.

6 Ice growth and melt over the Labrador Shelf

The coupled model can be used to investigate the dynamic and thermodynamical processes in ice covered ocean. As an example, the spatial variation of ice growth and melt rates over the Labrador Shelf in the 60 day period between mid-January and mid-March was calculated from a model run driven by climatological forcing (Fig. 8a) (Yao *et al.*, 2000a)[7]. The air-sea fluxes were computed from monthly climatology produced by NCEP/NCAR. Winds at 6 hour interval were used to derive monthly climatology of wind stress. Over the inner shelf, ice growth is positive. Over the outer shelf and slope, the growth is negative (i.e., ice melt) even though during this period the ice extent is increasing. This indicates that the increase in ice extent is not due to ice growth, but due to advection of ice from the north. The striking feature of Fig. 8a is the large melt along a narrow strip at the offshore ice edge. At the ice edge, melt typically exceeds 2 m (and exceeds 4 m in places) over the 60 day period, which is considerably larger than the thickness of the exiting ice.

The ice melt requires there to be an influx of ice for the location of the ice edge to be maintained. In Fig. 8b, the change in ice thickness from advection and diffusion of ice over the same period is shown. Over the inner shelf, there is divergence of the ice flux due to advection/diffusion; over the outer shelf, there is convergence of ice flux. The sign of the advection/diffusion term over most of the region opposes the sign of the growth. The magni-

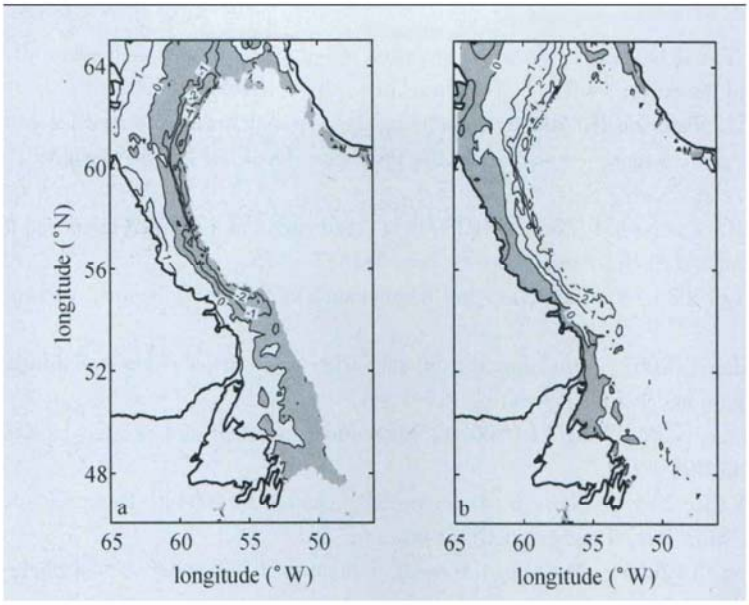

Fig. 8 (a) Ice growth between mid-January and mid-March. (b) Ice advection and diffusion between mid-January and mid-March. The contours are −2, −1, 0, 1, and 2 m. Out side this range the contour interval is 2 m. Negative regions are shaded. The figure is taken from Yao *et al.*, 2000a[7].

7 Summary and concluding remarks

A coupled ice-ocean model, CECOM, has been developed for Baffin Bay and the Labrador Sea. The sea-ice component of the model is a multi-category ice model in which mean concentration and thickness are expressed in terms of the thickness distribution function. Sea ice is coupled dynamically and thermodynamically to the Princeton Ocean Model. The coupled model has been used to study seasonal variation of sea ice and related ice-ocean processes, and transport and circulation in Baffin Bay and the Labrador Sea. The model has also been used in operational ice-ocean forecasting. Further development of the coupled model may include assimilation of available ice and ocean data, addition of a biological component, and improved specification of open boundary conditions. A future application of the model is to investigate the impacts of climate change on sea ice in eastern Canada's marginal ice zone. This is an area where intense economic activities including offshore oil production take place. Reliable predictions of ice conditions under climate change are required to manage the offshore resources effectively.

References

[1] Hibler WD(1979): A dynamic thermodynamic sea ice model. J. Phys. Oceanogr, 9:815 − 846.
[2] Ikeda M, Symonds G, Yao T(1988): Simulated fluctuations in annual Labrador Sea-ice cover. Atmosphere-Ocean, 26:16 − 39.
[3] Tang CL, Gui Q(1996): A dynamical model for wind-driven ice motion: application to ice drift on the Labrador Shelf. J. Geophys. Res., 101:28343 − 28364.
[4] Bryan K(1969): A numerical model for the study of the circulation of the world ocean. J. Comput. Phys., 4:347 − 376.
[5] Cox MD(1984): A primitive equation, 3-dimensional model of the ocean. Ocean Group Tech. Rep. 1, 143, Geophys. Fluid Dyn. Lab., Princeton, N. J.

[6] Ikeda M, Yao T, Yao Q(1996): Seasonal evolution of sea ice cover and shelf water off Labrador simulated in a coupled ice-ocean model. J. Geophys. Res., 101:16465 - 16490.

[7] Yao T, Tang CL, Peterson IK(2000a): Modeling the seasonal variation of sea ice in the Labrador Sea with a coupled multicategory ice model and the Princeton Ocean Model. J. Geophys. Res., 105:153 - 1165.

[8] Yao T, Tang CL, Carrieres T, Tran DH(2000b): Verification of a coupled ice ocean forecasting system for the Newfoundland Shelf. Atmosphere-Ocean, 38:557 - 575.

[9] Yao T, Tang CL(2003): The formation and maintenance of the North Water. Atmosphere-Ocean, 41: 187 - 201.

[10] Tang CL, Dunlap E(2007): Modeling the annual variation of sea-ice cover in Baffin Bay. International Journal of Offshore and Polar Engineering, 17:1 - 6.

[11] Dunlap E, Detracey BM, Tang CL(2007): Short-wave radiation and sea ice in Baffin Bay. Atmosphere-Ocean, 45:195 - 210.

[12] Tang CL, Ross CK, Yao T, Petrie B, Detracey BM, Dunlap E(2004): The circulation, water masses and sea-ice of Baffin Bay. Progress in Oceanogr., 63:183 - 228.

[13] Dunlap E, Tang CL(2006): Modeling the mean circulation of Baffin Bay. Atmosphere-Ocean, 44:99 - 110.

[14] Tang CL, Perrie W, Jenkins AD, Detracey BM, Hu Y, Toulany B, Smith PC(2007): Observation and modeling of surface currents on the Grand Banks - a study of the wave effects on surface current. J. Geophys. Res., 112:C10025, doi:10.1029/2006JC004028.

[15] Wang J, Liu Q, Jin M, Ikeda M, Saucier FJ(2005): A coupled ice-ocean model in the pan-Arctic and North Atlantic Ocean: simulation of seasonal cycles. J. Oceanogr., 61:213 - 233.

[16] Wang J, Wu B, Tang CL, Walsh JE, Ikeda M(2004): Sea saw structure of subsurface temperature anomalies between the Barents Sea and the Labrador Sea. J. Geophys. Res. Lett., 31:L19301, doi:10.1029/2004GL019981.

[17] Thorndike AS, Rothrock DA, Maykut GA, Colony R(1975): The thickness distribution of sea ice. J. Geophys. Res., 80:4501 - 4513.

[18] Hibler WD(1980): Modeling a variable thickness sea ice cover. Mon. Weather Rev., 108: 1843 - 1973.

[19] Mellor GL, Kantha LH(1989): An ice-ocean coupled model. J. Geophys. Res., 94:10,937 - 10, 954.

[20] Blumberg AF, Mellor GL(1987): A description of a three-dimensional coastal ocean circulation model. in Three-Dimensional Coastal Ocean Models. Coastal Estuarine Sci., 4, edited by N. S. Heaps, 1 - 16, AGU, Washington DC.

[21] Tang CL(2007): High-resolution monthly temperature and salinity climatologies for the northwestern North Atlantic Ocean. Canadian Data Report of Hydrography and Ocean Sciences, 169: 55.

[22] Martinsen EA, Engedahl H(1987): Implementation and testing of a lateral boundary scheme as an open boundary condition in a barotropic ocean model. Coastal Eng., 11: 603 - 627.